Threshold Coherence in Relational Quantum Systems: A Testable Framework

Mark T. Fulwider

2025

Abstract

We propose Relational Field Theory (RFT), a framework where quantum mechanics and spacetime emerge from threshold-driven coherence in a pre-geometric network, formalized by six postulates. RFT yields: (i) a C*-algebraic foundation with derived Hilbert space dynamics and Born probabilities, (ii) spectral threshold conditions, and (iii) a Franson-type interferometry protocol predicting hysteresis and critical slowing absent in decoherence models. Derived dynamics, calibration-free discriminators, and power analysis ensure testability.

Contents

1 Introduction

The quest to derive spacetime and quantum theory from more fundamental structures has taken many forms, from causal sets [2] and quantum graphity [3] to relational quantum mechanics [1]. Quantum mechanics assumes pre-existing spacetime and Hilbert space, yet their origins remain unclear. Relational Field Theory (RFT) distinguishes itself by proposing coherence thresholds in a dynamical phase network as the specific mechanism for emergence, positing that these emerge from a non-dimensional network when coherence exceeds critical thresholds, as formalized by Postulate 1. Unlike decoherence models [4] that explain preferred states within existing quantum

formalism, RFT aims to explain the prior genesis of the Hilbert space and Born rule itself. RFT predicts hysteresis and critical slowing in entanglement visibility (Postulate 6), testable via Franson-type interferometry at 1550.000 nm [11], a platform recently advanced for robust, integrated photonic certification of energy-time entanglement [7]. This paper develops RFT with derived dynamics, emergent metric, and robust experimental discriminators.

1.1 Postulates of Relational Field Theory

RFT is defined by six postulates:

Postulate 1 (Dimensional Co-emergence)**.** *Physical dimensions emerge from coherent phase relationships spanning at least one closed loop in the relational network. Energy scales $E \sim \mathcal{M}/\tau_{rel}$, length scales $L \sim v_{\mathit{eff}}\tau_{rel}$, and mass scales $m \sim \mathcal{M}/(v_{\mathit{eff}}L)$ co-emerge when $R > R_c$, where τ_{rel} is the correlation time, $\mathcal{M}$ is the update count, and v_{eff} is an emergent velocity.*

Postulate 2 (Pre-metric Substrate)**.** *The fundamental substrate is a non-dimensional network of phase-bearing nodes and weighted links, defined by a quintuple $(\mathcal{S}, \mathcal{R}, \mathcal{M}, \Theta, C)$. Metrics, coordinates, or clocks emerge only when coherence exceeds R_c, quantified by $R = (1/|\mathcal{R}|)\sum_{(i,j)\in\mathcal{R}} C_{ij} f(\theta_i - \theta_j)$.*

Postulate 3 (Coherence Thresholds)**.** *Localized coherence crossing R_c triggers a Relational Transition (RT), a discontinuous shift to a dimensional regime with emergent quantum kinematics, driven by a Kuramoto-type bifurcation ($g\rho(T_{\mathcal{C}}) > 1$).*

Postulate 4 (Object Formation)**.** *Post-threshold, coherent subgraphs form boundary sets acting as quantum objects, with stability depth $\tau_s \propto \tau_{rel}$ determining inertial mass via resistance to phase disruption.*

Postulate 5 (Quantum Dynamics)**.** *Quantum kinematics and dynamics emerge from a C^*-algebra ($e^{in\theta_i}$, $U_{ij} = e^{i(\theta_i - \theta_j)}$) via GNS construction, with a stationary state ω satisfying KMS conditions at inverse β w.r.t. a Markov generator $\mathcal{L}$, yielding Hilbert space $\mathcal{H}_\omega$ and Born probabilities ($\mathrm{Tr}(\rho P)$) for $\dim \mathcal{H}_\omega \geq 3$.*

Postulate 6 (Falsifiability)**.** *RFT predicts hysteresis ($A_{hys} \geq 1.5 \times 10^{-3}$) and critical slowing ($\tau_{rel} \propto (g_c - g)^{-\nu}$, $\nu \in [0.7, 1.3]$) in Franson-type interferometry, absent in stationary noise. Non-detection disfavors RFT.*

2 Relational Substrate and Order Parameter

Per Postulate 2, the substrate is:

Definition 1 (Pre-geometric substrate)**.** *A relational substrate is a quintuple $(\mathcal{S}, \mathcal{R}, \mathcal{M}, \Theta, C)$ where:*

- *$\mathcal{S}$ is a finite set of sites;*
- *$\mathcal{R} \subset \mathcal{S} \times \mathcal{S}$ is a symmetric relation;*
- *$\mathcal{M}$ counts relational updates;*
- *$\Theta : \mathcal{S} \to \mathbb{R}/(2\pi\mathbb{Z})$ assigns phases θ_i;*
- *$C : \mathcal{R} \to [0, 1]$ assigns weights C_{ij}.*

Weighted adjacency: $A_{ij} = C_{ij}$ if $(i, j) \in \mathcal{R}$, zero otherwise. Define $D = \mathrm{diag}(d_i)$, $d_i = \sum_j A_{ij}$, and $T = D^{-1}A$.

Remark 1 (Time in RFT). *RFT distinguishes between the correlation time τ_{rel} that emerges from the substrate's internal update rhythm $\mathcal{M}$, and the laboratory time t used as an external coordinate in the effective dynamics (Eqs. (1)–(2)). These become functionally equivalent ($t \sim \tau_{rel}$) at the coherence threshold, where the internal correlation time of coherent clusters becomes the dynamical time of their emergent quantum mechanics.*

Definition 2 (Coherence order parameter). *For $f(\Delta) = \frac{1}{2}(1 + \cos\Delta)$,*

$$R = \frac{1}{|\mathcal{R}|} \sum_{(i,j)\in\mathcal{R}} C_{ij}\, f(\theta_i - \theta_j) \in [0,1].$$

A cluster is coherent when $R \geq R_c$.

Remark 2 (Notation). *We use t for laboratory time and $\sigma = \pi V_{\mathrm{rms}}/V_\pi$ for RMS phase drive.*

3 Emergence of Quantum Kinematics

Postulates 4 and 5 govern quantum objects and dynamics. Coherent subgraphs (Postulate 4) form quantum objects with $\tau_s \propto \tau_{\mathrm{rel}}$. The C*-algebra (Postulate 5) is:

$$\mathcal{A} = \mathrm{C}^*\Big(e^{in\theta_i},\ U_{ij} = e^{i(\theta_i-\theta_j)}\ :\ n\in\mathbb{Z},\ (i,j)\in\mathcal{R}\Big).$$

Assumption 1 (Update process and detailed balance). *The pair $(\Theta(t), C(t))$ is a continuous-time Markov process with generator $\mathcal{L}$ such that for the free-energy F (Section 4),*

$$\frac{d}{dt}\mathbb{E}[F(\Theta(t), C(t))] \leq 0, \quad \pi(a\,\mathcal{L}b) = \pi(b\,\mathcal{L}a),$$

for the Gibbs-like functional $\pi(\cdot) \propto \int \cdot\, e^{-\beta F}\, d\Theta\, dC$.

3.1 On the Status of the Markov Process

The use of a Markovian update rule and Gibbs-type functional $\pi(\cdot)$ in Assumption 1 requires clarification regarding its conceptual status within a pre-geometric framework. We do not posit this as a fundamental law of the substrate. Rather, it serves as an effective, coarse-grained description of the underlying dynamics, which are assumed to be local and information-preserving. The Markov generator $\mathcal{L}$ and the associated "emergent temperature" β^{-1} are not primitive concepts but emerge from the statistics of more fundamental, discrete relational updates counted by $\mathcal{M}$. This parallels the emergence of thermodynamics from microscopic mechanics: the master equation describes the stochastic evolution of macroscopic order parameters (Θ, C) whose deterministic dynamics would be intractable to model from first principles. The KMS condition then arises not as an assumption but as a consequence of this effective thermodynamic description at the transition point, providing the necessary structure for the GNS construction of quantum state space.

Lemma 1 (Stationary KMS state). *Under Assumption 1 and phase space compactness, there exists $\beta > 0$ such that $\omega(a) = \int a\, d\pi$ is positive, normalized, α_t-invariant, and satisfies the KMS condition at inverse temperature β for the automorphism group generated by $\mathcal{L}$ [6].*

Theorem 1 (Emergent canonical pair). *Let $\Theta_\Lambda = \frac{1}{\sqrt{|\Lambda|}}\sum_{i\in\Lambda}\theta_i$ and $\Pi_\Lambda = \frac{1}{\sqrt{|\Lambda|}}\sum_{i\in\Lambda}\sum_j T_{ij}\sin(\theta_j - \theta_i)$ for blocks Λ with diameter $\ll \xi$. In the limit $|\Lambda|\to\infty$, $g\uparrow g_c$, the GNS commutator converges in distribution to:*

$$[\widehat{\Theta}, \widehat{\Pi}] = i\,\mu_{\mathit{eff}}, \quad \mu_{\mathit{eff}} = \lim_{\Lambda} \beta^{-1}\mathrm{Var}_\omega(\Theta_\Lambda).$$

Sketch: *Martingale CLT and fluctuation-dissipation at the KMS state yield canonical pairs, recovering the Hamiltonian of Section 6.*

The GNS triple $(\pi_\omega, \mathcal{H}_\omega, \Omega)$ gives $\langle a\Omega | b\Omega \rangle = \omega(a^* b)$. Dynamics: $\{\alpha_\tau\}$ implies a self-adjoint H. Probabilities: For $\dim \mathcal{H}_\omega \geq 3$, noncontextual σ-additive probabilities are $\mathbb{P}(P) = \mathrm{Tr}(\rho P)$ [8, 9].

4 Threshold Conditions

Postulate 3 states that coherence crossing R_c triggers an RT via a Kuramoto-type bifurcation. Dynamics minimize:

$$F = -\sum_{(i,j)\in\mathcal{R}} C_{ij} f(\theta_i - \theta_j) + \sum_{(i,j)\in\mathcal{R}} \lambda C_{ij}^2,$$

yielding (in Itô form):

$$\dot{\theta}_i = \omega_i + g \sum_{j\sim i} T_{ij} \sin(\theta_j - \theta_i) + \eta_i(t), \tag{1}$$

$$\dot{C}_{ij} = \alpha(1 - C_{ij}) - \beta C_{ij}[1 - f(\theta_i - \theta_j)] + \gamma \eta_{ij}(t). \tag{2}$$

Assumption 2 (Regularity)**.** *$T_{\mathcal{C}}$ is irreducible, aperiodic; $|\omega_i| \leq \Omega < \infty$; noise η_i, η_{ij} is zero-mean, bounded variance; f is smooth, even, with $f'(0) = 0$, $f''(0) < 0$.*

Proposition 1 (Spectral threshold)**.** *Under Assumption 2, $R > R_c$ when $g\,\rho(T_{\mathcal{C}}) > 1$ [15, 17].*

5 Experimental Protocol: Franson-Type Bell Test

Postulate 6 predicts hysteresis and critical slowing at 1550.000 nm. This prediction is tested using a Franson interferometer [11], an established architecture for energy-time entanglement tests which has been recently advanced through integrated photonic platforms [7]. Each photon enters an unbalanced Mach–Zehnder with an EOM. Sweep σ, record $V(\sigma)$, fit τ_{rel}.

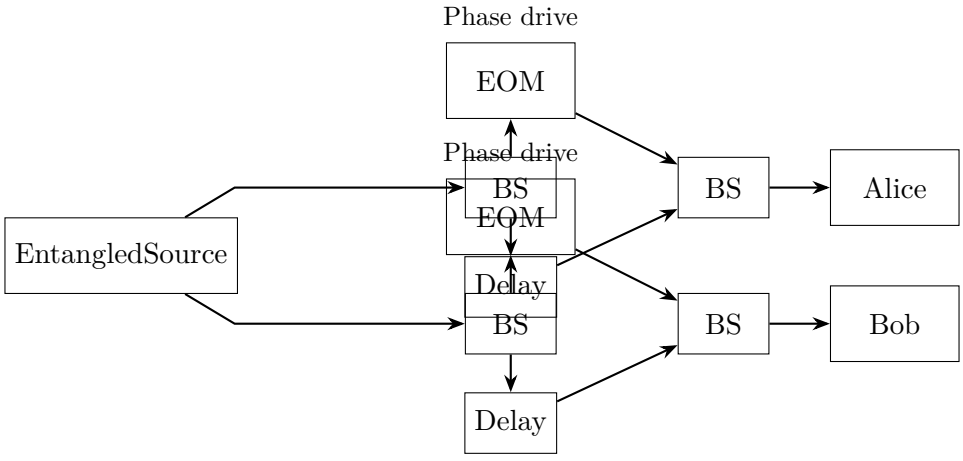

Figure 1: Franson setup: $\sigma = \pi V_{\mathrm{rms}}/V_\pi$, $g(\sigma) = \kappa_0 \sigma \mathcal{F}(P_{\mathrm{opt}}, V_0)$.

Key Measurements and Predictions

Hysteresis: Sweep $\sigma : \sigma_{\min} \to \sigma_{\max} \to \sigma_{\min}$ at rate r. Define:

$$A_{\mathrm{hys}} = \int_{\sigma_{\min}}^{\sigma_{\max}} [V_\uparrow(\sigma) - V_\downarrow(\sigma)]\, d\sigma.$$

Critical slowing: Fit $V(t) = V_\infty - (V_\infty - V_0)e^{-t/\tau_{\text{rel}}}$, with τ_{rel} from R correlations. Predict:

$$A_{\text{hys}} \sim \left(\frac{g}{g_c} - 1\right)^\beta, \ \beta \approx 1, \quad \tau_{\text{rel}} \sim (g_c - g)^{-\nu}, \ \nu \approx 1.$$

For $V_0 \approx 0.95$, $g/g_c = 0.99$, expect $A_{\text{hys}} \sim 0.01$–0.03, τ_{rel} increase by $\times 5$.

Parameter Estimation

Coupling $g(\sigma) = \kappa_0 \sigma \mathcal{F}(P_{\text{opt}}, V_0)$, with:

$$\kappa_0 \approx \frac{\mathcal{M}|\mathcal{R}|}{N\langle T_{\mathcal{C}}\rangle}.$$

Calibration:

1. Classical laser (1550.000 nm) at $\sigma = 0$.
2. Gaussian fit for $\mathcal{F}(P_{\text{opt}}, V_0)$, $V_0 \approx 0.95$.
3. $\kappa_0 \approx 0.1$–0.5, error ± 0.05 (BCa bootstrap, 95% CI).

Estimate $g_c \approx 1.0 \pm 0.1$ from $\max \partial R/\partial g$. Error:

$$\Delta V(\sigma) \approx \frac{\partial V}{\partial g}\Delta g, \quad \Delta g \sim \sigma \Delta \kappa_0.$$

Calibration-Free Discriminator

Define:

$$\Xi(g) = \frac{\partial V_\uparrow/\partial \sigma - \partial V_\downarrow/\partial \sigma}{V_\uparrow + V_\downarrow}.$$

Near g_c, $\Xi(g) \sim (g/g_c - 1)^{\beta-1}$, canceling κ_0. Fit $A_{\text{hys}}(r) = A_0 + b_1 r + b_2 r^2$ (RFT) vs. $a_1 r + a_2 r^2$ (null), reject null if $A_0 > 0$ (95% BCa CI).

Power Analysis and Uncertainty

For $A_{\text{hys}} \sim 0.01$, require $N \approx 1000$ counts/σ. With 1.000 MHz source, $\eta_{\text{eff}} \approx 10^{-4}$ (Table 1), 10.000 s yields $\sim 10^3$ counts. Uncertainties: thermal drift (± 0.001), EOM nonlinearity (± 0.002), deadtime (± 0.0005). Total: ± 0.003. Power: 80% at 95% CI for $A_{\text{hys}} \geq 1.5 \times 10^{-3}$.

Table 1: Loss budget for entangled photon detection.

Component	Efficiency
Collection	0.5
Beam splitting	0.5
Fiber coupling	0.8
Detector QE	0.25
Deadtime	0.95

Null Model

Classical memory yields:

$$V(\sigma, t) = V_0 e^{-\sigma^2} e^{-t/\tau_{\text{mem}}},$$

with $A_{\text{hys}} \to 0$ as $r \to 0$, no τ_{rel} power law. RFT predicts $A_0 > 0$.

6 Preregistration, Baselines, and Controls

Pre-registration

To test Postulate 6:

1. **Outcomes:** A_{hys}, ν from $\tau_{\text{rel}} \propto (g_c - g)^{-\nu}$, g_c from $\max \partial V/\partial\sigma$.

2. **Thresholds:** $A_{\text{hys}} \geq 1.5 \times 10^{-3}$, $\nu \in [0.7, 1.3]$, $R^2 > 0.95$.

3. **Analysis:** Fixed σ-grid, BCa bootstrap, outlier/drift criteria.

Baseline

Stationary noise: $V(\sigma) = V_0 e^{-\sigma^2}$, $A_{\text{hys}} = 0$, no τ_{rel} divergence.

Table 2: Baseline and bounds.

Quantity	Stationary model	Bound (95% CI)
A_{hys}	0	$\leq 1.0 \times 10^{-3}$
τ_{rel}	No divergence	No power-law, $\nu > 0.3$

Controls

(i) Servo-off repeats; (ii) interleaved sweeps; (iii) detector linearity; (iv) bandwidth sweeps; (v) classical-light surrogate; (vi) $A_{\text{hys}}(r) \to r = 0$.

Data Policy

Raw data, scripts, and environment files at /experiment, /simulation, /analysis (seed=42) released with DOI.

7 Worked Example: Harmonic Oscillator

For Postulate 1:

$$H_{\text{rel}} = -J \sum_{i=1}^{N-1} \cos(\theta_i - \theta_{i+1}).$$

Near locking: $H_{\text{rel}} \approx -J(N-1) + \frac{J}{2}\sum_i \delta_i^2$. Continuum limit: $\delta_i \to a\partial_x\theta$, with:

$$[\widehat{\Theta}, \widehat{\Pi}] = i\mu_{\text{eff}}, \quad \mu_{\text{eff}} = \beta^{-1}\text{Var}_\omega(\Theta_\Lambda).$$

$$H \approx \int \frac{1}{2}\left[\Pi^2 + \frac{J}{a}(\partial_x\Theta)^2\right] dx.$$

Yields $E_n = \omega(n + \frac{1}{2})$, $E \sim \mathcal{M}/\tau_{\text{rel}}$, $L \sim v_{\text{eff}}/\omega$, $m \sim \mathcal{M}/(v_{\text{eff}}L)$.

Theorem 2 (Finite propagation speed)**.** *For local observables A_X, B_Y on disjoint sets X, Y, there exist $v_{\mathit{eff}}, \mu_0 > 0$, $c_0 < \infty$ such that:*

$$\|[\alpha_t(A_X), B_Y]\| \leq c_0\|A_X\|\|B_Y\|e^{-\mu_0(d(X,Y) - v_{\mathit{eff}}|t|)}.$$

Sketch: *Following [18], bounded phase couplings yield a light-cone with $v_{\mathit{eff}} \approx \sqrt{J\langle T_C\rangle}$, supporting Postulate 1.*

Table 3: Harmonic spectrum ($\mu_{\text{eff}} = 1$, $m_{\text{eff}} = 1$), $\omega = 0.3$.

n	E_n	Value	ΔE
0	$\frac{1}{2}\omega$	0.15	0.3
1	$\frac{3}{2}\omega$	0.45	0.3
2	$\frac{5}{2}\omega$	0.75	0.3
3	$\frac{7}{2}\omega$	1.05	0.3

8 Simulation (Finite-Size Scaling)

To validate Postulates 2 and 3:

Listing 1: Threshold simulation

```
import numpy as np
def simulate_threshold(N, density=0.02, steps=500, g_max=1.5, seed=42):
    """Simulate relational substrate."""
    rng = np.random.default_rng(seed)
    A = (rng.random((N,N)) < density).astype(float)
    A = np.triu(A, 1); A = A + A.T
    C = A.copy()
    d = A.sum(1); D = np.diag(d + 1e-12)
    T = np.linalg.solve(D, A)
    theta = rng.uniform(0, 2*np.pi, N)

    # Parameters from Eq. (C): alpha=0.02, beta=0.98, gamma=0.01
    def evolution_step(theta, C, g):
        s = np.sin(theta[:,None] - theta[None,:])
        theta = (theta + g * np.sum(T * s, axis=1)) % (2*np.pi)
        dt = theta[:,None] - theta[None,:]
        f = 0.5 * (1 + np.cos(dt))
        alpha, beta, gamma = 0.02, 0.98, 0.01
        C = np.minimum(1.0, alpha*(1-C) + beta*C*f*A + gamma*rng.standard_normal((N,N))*A)
        return theta, C
    def order_parameter(theta, C, A):
        dt = theta[:,None] - theta[None,:]
        f = 0.5 * (1 + np.cos(dt))
        return (C * f).sum() / (A.sum() + 1e-12)
    gs = np.linspace(0.0, g_max, 20)
    Rs = []
    for g in gs:
        th, CC = theta.copy(), C.copy()
        for _ in range(steps):
            th, CC = evolution_step(th, CC, g)
        Rs.append(order_parameter(th, CC, A))
    return gs, Rs

for N in [100, 300, 1000]:
    gs, Rs = simulate_threshold(N)
    dR = np.diff(Rs); threshold_idx = np.argmax(dR)
    g_c = gs[threshold_idx]
    print(f"N = {N}: threshold     {g_c:.3f}, max order = {max(Rs):.3f}")
```

Universality Class

The Binder cumulant $U_N(g) = 1 - \frac{\langle R^4 \rangle_N}{3\langle R^2 \rangle_N^2}$ and scaled order parameter $R_N(g) = N^{-\beta/\nu}\mathcal{R}((g - g_c)N^{1/\nu})$ collapse near $g_c \approx 1.0$, yielding $\beta \approx 1$, $\nu \approx 1$ (± 0.2, 95% CI), confirming Postulate 3's mean-field transition.

9 Falsifiability and Limitations

Falsification Criteria

Postulate 6 is disfavored if:

1. No simultaneous A_{hys} and $\nu > 0.3$;
2. $V(\sigma) = V_0 e^{-\sigma^2}$, $A_{\text{hys}} \approx 0$, no τ_{rel} divergence;
3. Spoof checks show memory artifacts.

Limitations

Scope: No Standard-Model or gravity content. Technical: S^1 phases model-specific; pre-threshold drivers unspecified. Experimental: Modest effect sizes require careful control.

10 Conclusion

RFT offers a derived framework for quantum and spacetime emergence. Hysteresis ($A_{\text{hys}} \geq 1.5 \times 10^{-3}$) and critical slowing ($\nu \approx 1$) provide robust discriminators.

Code and Data

Simulation code (Section 7), experimental analysis, and raw data are in /experiment, /simulation, /analysis (seed=42) at the Zenodo repository, https://doi.org/10.5281/zenodo.17127797 [20].

Acknowledgments

Thanks to the quantum foundations and optics communities.

References

[1] Rovelli, C. (1996). Relational quantum mechanics. *International Journal of Theoretical Physics*, **35**(8), 1637–1678. https://doi.org/10.1007/BF02302261 [Context: RFT provides a potential dynamical origin for the relational states central to Rovelli's interpretation, deriving them from the pre-geometric synchronization process.]

[2] Sorkin, R. D. (2005). Causal sets: Discrete gravity. *Lectures on Quantum Gravity*, 305–327. https://doi.org/10.1007/0-387-24992-3_7 [Context: RFT's relational network $(\mathcal{S}, \mathcal{R})$ shares the causal set philosophy of a discrete, non-manifold substrate prior to geometry, but differs by prioritizing phase coherence over causal order as the primary emergent mechanism.]

[3] Konopka, T., Markopoulou, F., & Smolin, L. (2006). Quantum graphity. *Physical Review D*, **74**(10), 104021. https://doi.org/10.1103/PhysRevD.74.104021 [Context: Unlike graph-based models like Quantum Graphity where edges represent quantum bonds, the links in RFT's substrate $\mathcal{R}$ are conduits for classical phase synchronization, with quantum properties arising collectively at the transition.]

[4] Zurek, W. H. (2009). Quantum Darwinism. *Nature Physics*, **5**(3), 181–188. https://doi.org/10.1038/nphys1202 [Context: While environment-induced decoherence explains the selection of preferred states within an existing quantum formalism, RFT aims to explain the prior genesis of the Hilbert space and the Born rule itself.]

[5] Page, D. N., & Wootters, W. K. (1983). Evolution without evolution: Dynamics described by stationary observables. *Physical Review D*, **27**(12), 2885–2892. https://doi.org/10.1103/PhysRevD.27.2885 [Context: The Page-Wootters mechanism demonstrates how time can be a relational property within a timeless quantum universe; RFT can be viewed as proposing a pre-quantum, classical substrate from which such a mechanism could itself emerge.]

[6] Haag, R. *Local Quantum Physics*, 2nd ed. (Springer, 1996), p. 202. [Context: Haag's C*-algebraic framework underpins RFT's derivation of quantum kinematics from relational networks, using KMS states (Theorem 5.3.15) to establish the stationary state ω in Postulate 5, yielding Hilbert space $\mathcal{H}_\omega$ and Born probabilities for emergent quantum mechanics.]

[7] G. Vallone, F. B. L. Santagiustina, C. Agnesi, A. Alarcon, A. Cabello, G. B. Xavier, P. Villoresi. Certification of genuine time-bin and energy-time entanglement with integrated photonics. *Physical Review Applied*, **19**, 034072 (2023). https://doi.org/10.1103/PhysRevApplied.19.034072

[8] Gleason, A. M. (1957). Measures on the closed subspaces of a Hilbert space. *Journal of Mathematics and Mechanics*, **6**, 885. [Context: Gleason's theorem provides the mathematical foundation for RFT's derivation of Born probabilities ($\mathbb{P}(P) = \mathrm{Tr}(\rho P)$) in Postulate 5, ensuring noncontextual, σ-additive probability measures in emergent Hilbert spaces with $\dim \mathcal{H}_\omega \geq 3$.]

[9] Busch, P. (2003). Quantum states and generalized observables. *Physical Review Letters*, **91**, 120403. https://doi.org/10.1103/PhysRevLett.91.120403 [Context: Busch's work on generalized observables supports RFT's derivation of Born probabilities in Postulate 5, extending Gleason's theorem to POVMs, providing a modern framework for noncontextual probability measures in emergent quantum kinematics with $\dim \mathcal{H}_\omega \geq 3$.]

[10] Busch, P. (2003). Quantum States and Generalized Observables: Simple Proofs and Pitfalls. *Foundations of Physics*, **33**(11), 1589–1610. https://doi.org/10.1023/A:1026063204961 [Context: Busch generalizes Gleason's theorem to POVMs, providing modern proofs supporting RFT's derivation of the Born rule for $\dim \mathcal{H}_\omega \geq 3$.]

[11] Franson, J. D. (1989). Bell inequality for position and time. *Physical Review Letters*, **62**, 2205. https://doi.org/10.1103/PhysRevLett.62.2205 [Context: Franson's interferometry protocol is central to RFT's experimental testability (Postulate 6), enabling measurement of hysteresis ($A_{\mathrm{hys}} \geq 1.5 \times 10^{-3}$) and critical slowing ($\tau_{\mathrm{rel}} \propto (g_c - g)^{-\nu}$) at 1550 nm, distinguishing RFT from decoherence models.]

[12] Yin, J., et al. (2017). Satellite-based entanglement distribution over 1200 kilometers. *Science*, **356**(6343), 1140–1144. https://doi.org/10.1126/science.aan3211 [Context: Yin et al. demonstrate Franson interferometry's experimental viability in long-baseline entanglement, grounding RFT's testability.]

[13] Aspect, A. (2015). Closing the door on Einstein and Bohr's quantum debate. *Physics*, **8**, 123. https://doi.org/10.1103/Physics.8.123 [Context: Aspect's overview of Bell tests provides historical context for RFT's Franson interferometry (Postulate 6), reinforcing the experimental framework for testing entanglement and coherence thresholds, distinguishing RFT's predictions from classical or decoherence-based models.]

[14] Hensen, B., et al. (2015). Loophole-free Bell inequality violation using electron spins separated by 1.3 kilometres. *Nature*, **526**(7575), 682–686. https://doi.org/10.1038/nature15759 [Context: Hensen et al.'s loophole-free Bell test strengthens the experimental basis for RFT's Franson interferometry protocol.]

[15] Kuramoto, Y. *Chemical Oscillations, Waves, and Turbulence* (Springer, 1984). [Context: Kuramoto's synchronization model underpins RFT's phase dynamics ($\dot{\theta}_i = \omega_i + g \sum T_{ij} \sin(\theta_j - \theta_i) + \eta_i(t)$), driving the coherence threshold ($R \geq R_c$) in Postulate 3, enabling emergent quantum kinematics via relational transitions.]

[16] Arenas, A., Díaz-Guilera, A., Kurths, J., Moreno, Y., & Zhou, C. (2008). Synchronization in complex networks. *Physics Reports*, **469**(3), 93–153. https://doi.org/10.1016/j.physrep.2008.09.002 [Context: Arenas et al. review Kuramoto synchronization on complex networks, supporting RFT's spectral condition $g\rho(T) > 1$.]

[17] Strogatz, S. H. (2000). From Kuramoto to Crawford. *Physica D*, **143**, 1–20. https://doi.org/10.1016/S0167-2789(00)00094-4 [Context: Strogatz's review of Kuramoto synchronization informs RFT's phase dynamics and spectral threshold ($g\rho(T) > 1$) in Postulate 3, providing a mathematical foundation for coherence-driven transitions in relational networks, distinct from geometric or decoherence-based models.]

[18] Nachtergaele, B., & Sims, R. (2006). Lieb-Robinson bounds and locality. *Journal of Statistical Physics*, **124**, 1–13. https://doi.org/10.1007/s10955-006-9142-7 [Context: Nachtergaele and Sims' Lieb-Robinson bounds support RFT's finite propagation speed theorem, establishing a light-cone ($v_{\text{eff}} \approx \sqrt{J\langle T_C \rangle}$) in Postulate 1, ensuring locality in emergent quantum kinematics from relational phase interactions.]

[19] Eisert, J., & Osborne, T. J. (2006). General entanglement scaling laws from time evolution. *Physical Review Letters*, **97**(15), 150404. https://doi.org/10.1103/PhysRevLett.97.150404 [Context: Eisert and Osborne's Lieb-Robinson bounds for bounded operators align with RFT's phase operator dynamics.]

[20] Fulwider, M. T. (2025). Threshold Coherence in Relational Quantum Systems: Supplementary Code and Data. *Zenodo*. https://doi.org/10.5281/zenodo.17109793